Covariance Based Image Selective Segmentation Model

Haider Ali*
Ghulam Murtaza*
Noor Badshah*
Department of Basic Sciences, UET Peshawar.

ABSTRACT

Many variational models for image segmentation can be seen in the literature and most of them uses image data fidelity term which involves a given image information only. Usually an energy functional for such models consist two energy functionals namely, external energy and internal energy. External energy helps to attracts the active contour towards the true boundaries of an object, whereas internal energy help to maintain the smoothness of the dynamic curve. In region based models of image segmentation, the external energy is usually the data fidelity term. In this paper we proposed a new variational model of image selective segmentation which utilizes given image information as well as information from an enhanced version of the given image. Experimental results on some real and synthetic images validate the efficiency and robustness of our proposed model in a very few iteration.

Keywords : Segmentation, Covariance (CoV), Level Set, Functional Minimization, Total Variation (TV).

1. INTRODUCTION

Image segmentation is an important branch of image processing. Segmentation of images means to divide an image into its constituent parts which are homogeneous in some sense like intensity or texture etc.

Many variational models have been developed for image segmentation problem and few examples are, minimum description length criteria [8] ,watershed algorithms [15], region growing and emerging [1] and Mumford-Shah functional minimization [10].

Let $u(x,y)$ be a given image defined on a rectangular domain Ω. Mumford and Shah (MS) proposed general model:

$$\min_{I,\Gamma} F(I,\Gamma) = \mu.length(\Gamma) + \lambda \int_{\Omega} |u - I|^2 dx + \int_{\Omega \setminus \Gamma} |\nabla I|^2 dx.$$

to automatically detect edge Γ of u and piecewise smooth version I of u. The Chan-Vese (CV) proposed the following model [3]:

$$
\begin{aligned}
F(\phi, t_1, t_2) &= \mu \int_{\Omega} \delta(\phi)|\nabla \phi| dx dy + \lambda_1 \int_{\Omega} |u(x,y) - t_1|^2 H(\phi) dx dy \\
&+ \lambda_2 \int_{\Omega} |u(x,y) - t_2|^2 (1 - H(\phi)) dx dy,
\end{aligned}
\tag{1}
$$

where ϕ is a level set function [12, 13], $\delta(\cdot)$ is the Dirac delta function and $H(\cdot)$ is the Heaviside function. where u is a given image, t_1 and t_2 are constants denoting average values of u inside and outside of Γ respectively. Although MS and CV models work efficiently for several segmentation tasks, but sometimes we are not interested to segment the whole image but only need to segment the single part from the whole image, this process of segmenting the single region among the several region of an image classify as image selective segmentation.

Recently, we proposed [2] a new model of selective segmentation, which is discussed in next section.

In contrast with existing models, there we ensured the better performance of our model in noisy images and best efficiency in terms of robustness and accuracy. In images with low contrast, intersecting regions with homogeneous intensities and in images having un-illuminated objects, the Badsha-Chen [2] model may fails to work. Now we will equip our model with a new type of image data fidelity term that can work better even when a given image has overlapping regions with almost homogeneous intensities or when edges of a given image are not prominent. This data fidelity term is based on the concept of covariance. Our experimental results show the stupendous performance of this new type of fidelity term based model, in contrast with the old model.

We organize this paper in the following way. In section 2 we give a review of the Badshah-Chen model [2]. In section 3 we introduce our proposed new variational model of minimization and the corresponding Euler-Lagrange equation. In Section 4 we include an additive operator splitting (AOS) scheme for solving the PDE. In Section 5 we include some experimental results.

2. THE BADSHAH-CHEN MODEL (BC)

To segment a given image *u*, The Badshah and Chen Model [2] is

$$\min_{t_1,t_2,\Gamma} F(\Gamma, t_1, t_2)$$

where

$$
\begin{aligned}
F(\Gamma, t_1, t_2) &= \mu \int_{\Gamma} d(x,y) g(|\nabla u|) ds \\
&+ \lambda_1 \int_{outside(\Gamma)} (u - t_1)^2 dx dy + \lambda_2 \int_{inside(\Gamma)} (u - t_2)^2 dx dy
\end{aligned}
\tag{2}
$$

& μ, λ_1 and λ_2 are positive parameter, t_2 and t_1 are the average intensities inside and outside a contour Γ respectively. The function $d(x, y)$ is a distance function defined in [6] as:

$$d(x,y) = \prod_{i=1}^{n}\left(1 - e^{-\frac{(x-x_i)^2}{2\sigma^2}} e^{-\frac{(y-y_i)^2}{2\sigma^2}}\right), \qquad \forall (x,y) \in \Omega,$$

where the marker set

$$A = \{(x_i, y_i) : i = 1, 2, 3, \ldots, m\}$$

are the given geometrical constraints and we want that the boundary of an object of interest to be detected.

$g(|\nabla u|)$ is denoting edge detector function and the following one is a popular choice.

$$g(|\nabla u|) = \frac{1}{1 + |\nabla u|^2}$$

In level set formulation, equation (2) becomes

$$
\begin{aligned}
F(\phi, t_1, t_2) &= \mu \int_{\Omega} d(x,y) g(|\nabla u|)\delta(\phi)|\nabla\phi|dxdy + \lambda_1 \int_{\Omega} |u(x,y) - t_1|^2 H(\phi)dxdy \\
&\quad + \lambda_2 \int_{\Omega} |u(x,y) - t_2|^2 (1 - H(\phi))dxdy,
\end{aligned}
$$

where

$$H(x) = \begin{cases} 1 & \text{if } x \geq 0 \\ 0 & \text{if } x < 0 \end{cases} \qquad \text{and} \qquad \delta(x) = H'(x)$$

are the one dimensional Heaviside and Dirac delta function respectively.
Since the Heaviside function is not derivable at the origin, a regularized version of Heaviside function is used [3, 4, 11],

$$H_\epsilon(z) = \frac{1}{2}\left(1 + \frac{2}{\pi}\arctan\left(\frac{z}{\epsilon}\right)\right), \qquad \delta_\epsilon(z) = H_\epsilon'(z) = \frac{\epsilon}{\pi(\epsilon^2 + z^2)}.$$

The regularized functional $F_\epsilon(\phi, t_1, t_2)$, is given by

$$
\begin{aligned}
F_\epsilon(\phi, t_1, t_2) &= \mu \int_{\Omega} d(x,y) g(|\nabla u|)\delta_\epsilon(\phi)|\nabla\phi|dxdy + \lambda_1 \int_{\Omega} |u(x,y) - t_1|^2 H_\epsilon(\phi)dxdy \\
&\quad + \lambda_2 \int_{\Omega} |u(x,y) - t_2|^2 (1 - H_\epsilon(\phi))dxdy.
\end{aligned}
$$

Keeping ϕ fixed and minimizing $F_\epsilon(\phi, t_1, t_2)$ with respect to t_1 and t_2, we have

$$t_1(\phi) = \frac{\int_{\Omega} u(x,y) H_\epsilon(\phi)dxdy}{\int_{\Omega} H_\epsilon(\phi)dxdy}, \quad t_2(\phi) = \frac{\int_{\Omega} u(x,y)(1 - H_\epsilon(\phi))dxdy}{\int_{\Omega}(1 - H_\epsilon(\phi))dxdy},$$

assuming that the curve has a non-empty interior and non-empty exterior in Ω. Keeping t_1, t_2 fixed and minimizing F_ϵ with respect to ϕ gives the following Euler-Lagrange equation for ϕ :

$$
\begin{cases}
\delta_\epsilon(\phi)\left[\mu \text{div}\left(W(x,y)\frac{\nabla\phi}{|\nabla\phi|}\right)\right. \\
\left. -\lambda_1(u(x,y) - t_1)^2 + \lambda_2(u(x,y) - t_2)^2\right] = 0 & \text{in } \Omega, \\
\dfrac{W(x,y)\delta_\epsilon(\phi)}{|\nabla\phi|}\dfrac{\partial\phi}{\partial\vec{n}} = 0 & \text{on } \partial\Omega,
\end{cases}
\tag{3}
$$

where

$$W(x,y) = d(x,y)g(|\nabla u|),$$

$\vec{n}$ is the unit exterior normal to the boundary $\partial\Omega$, and $\dfrac{\partial\phi}{\partial\vec{n}}$ is the normal derivative of ϕ at the boundary.

The above PDE may be considered as a steady state form of the following evolution equation:

$$
\begin{aligned}
\frac{\partial\phi}{\partial t} &= \delta_\epsilon(\phi)\Big[\mu\nabla.\Big(W(x,y)\frac{\nabla\phi}{|\nabla\phi|}\Big) \\
&\quad - \lambda_1(u-t_1)^2 + \lambda_2(u-t_2)^2\Big], \quad in\ \Omega \\
\phi(t,x,y) &= \phi_0(x,y), \quad in\ \Omega.
\end{aligned}
\tag{4}
$$

A balloon term [6], $\alpha W(x,y)|\nabla\phi|$, was added for speed the convergence of the model and iteration initialization, where α is a constant. We use the Additive Splitting scheme [17, 9] to solve the above evolution equation.
Since the function

$$\int_\Gamma d(x,y)g(|\nabla u|)ds \tag{5}$$

similar to [5, 6], is the first term of Badshah-Chen model. The purpose of this model was to minimize their proposed functional so that to find the unknown boundary curve f_i. but in case of noisy image it is difficult for an edge detector function in detecting edges. As this model based on edge detector function so it is oftenly fails to work in case of noisy images and in images with fuzzy edges. Isotropic Gaussian smoothing helps in smoothing u, but unfortunately it also smooth the edges. The second term of BC model is the image data fidelity term $\int_{outside(\Gamma)}(u-t_1)^2 dxdy + \int_{inside(\Gamma)}(u-t_2)^2 dxdy$ which belongs to the

CV model proposed in [3]. This term facilitate the BC model to work in noisy images and to obtain fast convergence in terms of number of iteration.

However there are images which are challenging for selective segmentation problem. In particular, CT and MRI images with unilluminated organs, fuzzy edges, and overlapping homogeneous regions.

Since the BC model (2) involves the fidelity term or region detector $\int|u-t_1|^2 dxdy + \int|u-t_2|^2 dxdy$ taken from CV model [3]. our experimental results shows that BC model does not work well, while working with such challenging images due to detection of spurious objects. For segmenting such tough and challenging images in selective segmentation task ,better region detectors are required. To fulfill these requirement, here we proposed our covariance based selective segmentation model.

3. THE PROPOSED MODEL

In this section we will present our new variational model for image selective segmentation and will compare our proposed model with the latest existing models [2, 5]

Since a fidelity term usually carries a given image information only and many models can be seen in the literature with such fidelity terms [2, 3, 7, 14, 16].

The idea of covariance can help to robust an energy functional which consist statistical information of a given image as well as it incorporates guidance from an enhanced version of that image.

Since covariance of two variables *A* and *B*, is given by:

or

$$C = \frac{1}{n-1} \sum \left(A - \overline{A} \right)\left(B - \overline{B} \right),$$

$$C = \frac{1}{n-1} \sum \left(AB - \overline{A}\,\overline{B} \right). \tag{6}$$

Along with a given image $I_0(x, y)$, we wish to use as an enhanced version of $I_0(x, y)$, the averaging convolution image $I^*(x, y)$, i.e.,

$$I^*(x, y) = p_k * I_0(x, y),$$

with p_k an averaging convolution operator of window size $k \times k$.

The equation (6) can help to construct a fidelity term in continuous settings that can include, a given image information and incorporates information of a enhanced version of the image, in the main model.

Thus we construct a fidelity term by using L^2 norm and therefore the product of means can be replaced by a constant (say) t_i by observing (6).

We get:

$$\int_{outside(\Gamma)} (II^* - t_1)^2 dxdy + \int_{inside(\Gamma)} (II^* - c_2)^2 dxdy. \tag{7}$$

Usually in region-based models two terms namely, global term and local term, contribute mainly. A global term helps in detecting the main structure formed by objects/regions in an image, where as, a local term helps in capturing small and valuable details. For utilizing local information, we use local fitting term proposed in [7] given by,

$$\int_{outside(\Gamma)} \left((p_k * u - u) - c_1 \right)^2 dxdy + \int_{inside(\Gamma)} \left((p_k * u - u) - c_2 \right)^2 dxdy, \tag{8}$$

where p_k an averaging convolution operator of window size $k \times k$, c_1 and c_2 are the average intensities of the difference image $(p_k * u - u)$ inside and outside Γ, respectively and $u = II^*$.

By denoting the difference image $(p_k * u - u)$ with u^*, so to develop our new model, we combine the fitting terms given in (7) and (8) with the function given in (5) as follows:

$$
\begin{aligned}
F(\Gamma, t_1, t_2, c_1, c_2) \;=\; & \mu \int_{\Gamma} d(x, y) g(|\nabla u|) ds \\
& + \int_{outside(\Gamma)} \left[\lambda_1 (II^* - t_1)^2 + \lambda_2 (u^* - c_1)^2 \right] dxdy \\
& + \int_{inside(\Gamma)} \left[\lambda_1 (II^* - t_2)^2 + \lambda_2 (u^* - c_2)^2 \right] dxdy.
\end{aligned}
\tag{9}
$$

Since the *F* model involves data fidelity terms that incorporates both local and global information. Therefore, for the comparison with the latest existing selective segmentation models [2, 5], we prefer to use the *F* model in next experimental section. For simplicity, we give briefly only the minimization of *F* here.
The *F* in level set formulation is given by:

$$
\begin{aligned}
F(\phi, t_1, t_2, c_1, c_2) &= \mu \int_\Omega d(x,y) g(\mid \nabla u \mid) \delta(\phi) |\nabla \phi| dx dy \\
&+ \int_\Omega \Big[\lambda_1 (u - t_1)^2 + \lambda_2 (u^* - c_1)^2 \Big] H(\phi) dx dy \\
&+ \int_\Omega \Big[\lambda_1 (u - t_2)^2 + \lambda_2 (u^* - c_2)^2 \Big] (1 - H(\phi)) dx dy,
\end{aligned}
$$

where μ, λ_1 and λ_2 are constants and are used for assigning different weights.

By considering the following regularized minimization problem
min

$$
\min_{\phi, t_1, t_2, c_1, c_2} F_\epsilon(\phi, t_1, t_2, c_1, c_2),
$$

where

$$
\begin{aligned}
F_\epsilon(\phi, t_1, t_2, c_1, c_2) &= \mu \int_\Omega d(x,y) g(\mid \nabla u \mid) \delta_\epsilon(\phi) |\nabla \phi| dx dy \\
&+ \int_\Omega \Big[\lambda_1 (u - t_1)^2 + \lambda_2 (u^* - c_1)^2 \Big] H_\epsilon(\phi) dx dy \\
&+ \int_\Omega \Big[\lambda_1 (u - t_2)^2 + \lambda_2 (u^* - c_2)^2 \Big] (1 - H_\epsilon(\phi)) dx dy,
\end{aligned}
$$

minimization of $F_\epsilon(\phi, t_1, t_2, c_1, c_2)$ with respect to t_1, t_2, c_1, c_2 and ϕ leads to the following solutions:

$$
t_1(\phi) = \frac{\int_\Omega u(x,y) H_\epsilon(\phi) dx dy}{\int_\Omega H_\epsilon(\phi) dx dy}, \quad t_2(\phi) = \frac{\int_\Omega u(x,y)(1 - H_\epsilon(\phi)) dx dy}{\int_\Omega (1 - H_\epsilon(\phi)) dx dy},
$$

$$
c_1(\phi) = \frac{\int_\Omega u^*(x,y) H_\epsilon(\phi) dx dy}{\int_\Omega H_\epsilon(\phi) dx dy}, \quad c_2(\phi) = \frac{\int_\Omega u^*(x,y)(1 - H_\epsilon(\phi)) dx dy}{\int_\Omega (1 - H_\epsilon(\phi)) dx dy},
$$

and ϕ :

$$
\begin{cases}
\delta_\epsilon(\phi) \Big[\mu \mathrm{div} \Big(W(x,y) \dfrac{\nabla \phi}{|\nabla \phi|} \Big) \\
+ \lambda_1 \Big(-(u - t_1)^2 + (u - t_2)^2 \Big) + \lambda_2 \Big(-(u^* - c_1)^2 + (u^* - c_2)^2 \Big) \Big] = 0 & \text{in } \Omega, \quad (11) \\
\dfrac{\partial \phi}{\partial \vec{n}} = 0 & \text{on } \partial \Omega,
\end{cases}
$$

where $\vec{n}$ is an exterior unit normal to the boundary $\partial \Omega$ and $\dfrac{\partial \phi}{\partial \vec{n}}$ is the normal derivative

of ϕ at the boundary. The above PDE may be considered as a steady state form of the following evolution equation.

$$
\begin{aligned}
\frac{\partial \phi}{\partial t} &= \delta_\epsilon(\phi) \Big[\mu \nabla \cdot \Big(W(x,y) \frac{\nabla \phi}{|\nabla \phi|} \Big) - \lambda_1 (u - t_1)^2 \quad\quad\quad (12) \\
&- \lambda_2 (u^* - c_1)^2 + \lambda_2 (u - t_2)^2 + \lambda_2 (u^* - c_2)^2 \Big], \;\; in \; \Omega \\
\phi(x,y,t) &= \phi_0(x,y,0), \;\; in \; \Omega.
\end{aligned}
$$

By implementing, AOS method as done in [9, 17, 18] to solve the PDE (12), the following system of equations is obtained.

$$(I - 2\Delta t D_l(\Phi^p))\Phi_l^{p+1} = f^p, for\ l = 1, 2,$$

$$and\ \Phi_l^{p+1} = \frac{1}{2}\sum_{l=1}^{2}\Phi_l^{p+1},$$

where I is the identity matrix and $D_l\ for\ l = 1, 2$ a tridiagonal matrix.

4. EXPERIMENTAL RESULTS

In this section we give some simulation results. For convenience, we shall denote by
M-1 . the Gout model
M-2 . the BC model and
M-3 . the proposed CLM.

Below we give comparison results of these three methods.
In both M-2 and M-3, we use $\lambda_1 = \lambda_2 = \lambda$.

The behavior of M-2 can be seen in figures 1(c) and 2(c). On the other hand the following experiments reveal the failure of M-1 model. In figures 1(b) and 2(b) it can be seen that M-1 did not completed the tasks. In contrast with M-1, M-2, the best performance of M-3 can be seen from the experiments. The experiments also exhibit that M-3 is best in accurate and fast detection and successful in the images in which these two models are unable to work.

In figure 1(d) and 2(d) the successful detection by M-3 can be easily seen.

In summary, it has been observed from the experiments that, while performing selective segmentation on the challenging images having nearly equal intensity regions or fuzzy edges, the performance of M-2 is less effective, as in such cases it is often observed that the active contour crosses the boundary of an object of interest in the image and therefore the existing model is unable in detecting the actual boundary and consequently the region of interest in the image. In contrast, the proposed new M-3 outperforms all existing methods.

In summary a new image selective segmentation model is proposed which utilize both local and global information of a given image. Experimental results validate that this new model is robust in terms of accurate detection than the existing models.

Fig. 1
Segmenting a synthetic image using the proposed M-3 method: (a)initial contour; (b)Result of M-1; (c)Result of M-2 (d) Result of M-3, size=256 X 256
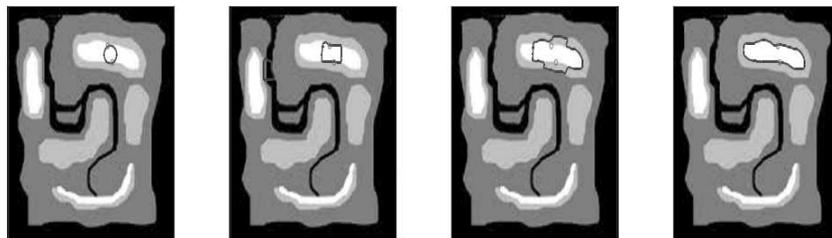
(a) Initial Contour   (b) Result of M-1   (c) Result of M-2   (d) Result of M-3

Fig. 2
Successful detection of selected portion in real heart image by the proposed M-3 can be seen in gure 2(d). In contrast with M-3, the uncompleted tasks by M-1 and M-2 can also be seen clearly in 2(b) and 2(c).
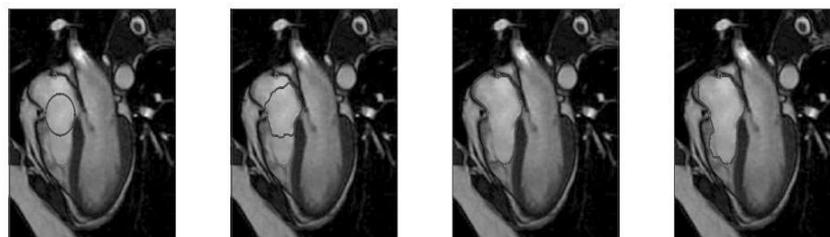
(a) Initial Contour   (b) Result of M-1   (c) Result of M-2   (d) Result of M-3

REFERENCES

[1] R. Adams and L. Bischof. Seeded region growing. IEEE Trans. Pattern Analysis and-Machine Intelligence, 16(6):641-647, 1994.

[2] N. Badshah and K. Chen. Image Selective Segmentation under Geometrical Constraints Using an Active Contour Approach. Math. Comp., 7:759.778, 2010.

[3] T. F. Chan and L. A. Vese. Active contours without edges. IEEE Transactions on Image Processing, 10(2):266.277, 2001.

[4] K. Chen. Matrix Preconditioning Techniques and Applications. Cambridge University Press, 2005.

[5] C. Gout, C. L. Guyader and L. A. Vese. Segmentation under geometrical conditions with geodesic active contour and interpolation using level set method. Numerical Algorithms, 39:155-173, 2005.

[6] C. L. Guyader and C. Gout. Geodesic active contour under geometrical conditions theory and 3D applications. Numerical Algorithms, 48:105-133, 2008.

[7] X. F. Wang, D. S. Huang, H. Xu. An efficient local Chan-Vese model for image segmentation. Pattern Recognition , 43:603.618, 2010.

[8] Y. Leclerc. Region growing using the MDL principle, In: DAPPRA Image Understanding Workshop, 1990.

[9] T. Lu, P. Neittaanmaki, and X. C. Tai. A parallel splitting up method and its application to Navier-Stokes equations Appl. Math. Lett., 4(2):25-29, 1991. 10 Covariance Based Image Selective Segmentation Model

[10] D. Mumford and J. Shah. Optimal approximation by piecewise smooth functions and associated variational problems. Communications on Pure Applied Mathematics, 42:577.685, 1989.

[11] S. Osher and R. Fedkiw $f_¡$-Level Set Methods and Dynamic Implicit Surfaces, Springer Verlag, 2003 Lec. Notes Comp. Sci., 3708:499-506, 2005.

[12] S. Osher and J. A. Sethian. Fronts propagating with curvature-dependent speed: algorithms based on Hamilton-Jacobi formulations. J. Comput. Phys., 79(1):12.49, 1988.

[13] J. A. Sethian Level set methods and fast marching methods. Evolving interfaces in Computational Geometry, Fluid Mechanics, Computer Vision and Material Science, Cambridge University Press, 1999.

[14] L. A. Vese and T. F. Chan. A multiphase level set framework for image segmentation using the Mumford and Shah model, Int. J. Computer Vision, 50(3):271-293, 2002.

[15] L. Vincent and Soille. Watersheds in Digital Spaces - an efficient algorithm based on immersion. IEEE Trans. Pattern Analysis and Machine Learning, 6:583-598, 1994.

[16] L. Wang, C. Li, D. Xia, C. Y. Kao. Active contour driven by local and global intensity fitting energy with application to brain MR image segmentation. Computerized Medical Imaging and Graphics, 33:520-531, 2009.

[17] J. Weickert, B. M. ter Haar Romeny and M. A. Viergever. Efficient and reliable schemes for nonlinear diffusion filtering, IEEE Trans. Image Proc., 7:398-410, 1998.

[18] J. Weickert and G. Kuhne. Fast methods for implicit active contours models. In: Geometric Level SetMethods in Imaging, Vision, and Graphics, pp.43-58, 2003.